Available online at www.sciencedirect.com

SciVerse ScienceDirect

Procedia CIRP 8 (2013) 378 – 383

www.elsevier.com/locate/procedia

14th CIRP Conference on Modeling of Machining Operations (CIRP CMMO)

Influence of the Material Behavior Law and Damage Value on the Results of an Orthogonal Cutting Finite Element Model of Ti6Al4V

F. Ducobu*, E. Rivière-Lorphèvre, E. Filippi

University of Mons (UMONS), Faculty of Engineering (FPMs), Machine Design and Production Engineering Department, 20 Place du Parc, B-7000 Mons (Belgium)

* Corresponding author. Tel.: +32 65 37 45 47; fax: +32 65 37 45 45. *E-mail address*: Francois.Ducobu@umons.ac.be.

Abstract

A finite element model has been developed with Abaqus/Explicit to model the orthogonal cutting of Ti6Al4V. Experiments were carried out to validate its results. The experimental cutting conditions are the same as those used in the finite element model. They lead to the production of a saw-toothed chip, either numerically or experimentally. The comparison of the model results shows that the difference with the experimental RMS cutting force value is quite large (about 40%). Both chips morphologies are similar although the teeth of the simulated one have smaller valleys and lengths. The numerical model could therefore be improved. The aim of this paper is to study the influence of the material behavior law and the damage value on the model results, in order to get closer to the experimental results. It shows that the difference between numerical and experimental cutting forces reduces drastically (it becomes of the order of 2%) for stresses obtained with the modified behavior law similar to those observed in the literature. The teeth of the chip have a larger valley and are therefore closer to the experimental chip. These improvements do not interfere with the physics of the saw-toothed chip formation, which is still the same as the experimental one. An important point is that it turns out that the influence of the material behavior law and of the damage value are almost decoupled within the limits of the variations selected. Indeed, the material behavior law controls the level of the cutting force while the damage value acts mostly on the morphology.

Selection and peer-review under responsibility of The International Scientific Committee of the "14th CIRP Conference on Modeling of Machining Operations" in the person of the Conference Chair Prof. Luca Settineri

Keywords: Chip formation; damage; finite element; material behavior law; saw-toothed chip; Ti6Al4V

1. Introduction

Modeling of machining processes is nowadays widely used, in addition to experiments, to provide a better understanding of cutting mechanics. It also reduces costs by limiting the number of experiments and provides access to hard-to-measure values such as temperatures or residual stresses. Machining is a complex process, making it difficult to be modeled. The model development involves many parameters influencing the results.

This paper shows the comparison between modeling and experimental results. Some differences will be highlighted and the influence of the material behavior law and damage value on the results will be studied. The machined material is Ti6Al4V, a titanium alloy often used in aeronautical and biomedical applications. It is known to be a difficult-to-machine material producing saw-toothed chips for some cutting conditions.

2. Numerical model presentation

The numerical model used in this study is the Lagrangian Finite Element Method (FEM) model presented in [1] to study the influence of the depth of cut on chip formation in 2D plain strain orthogonal cutting of Ti6Al4V. It was developed with the commercial software ABAQUS/Explicit.

As for the experiments, the cutting tool is modeled with a finite edge radius of 20 µm, its rake and clearance angles are equal, respectively, to 15° and 2°. Fig. 1 shows the initial geometry and boundary conditions of

Selection and peer-review under responsibility of The International Scientific Committee of the "14th CIRP Conference on Modeling of Machining Operations" in the person of the Conference Chair Prof. Luca Settineri
doi:10.1016/j.procir.2013.06.120

the model. The cutting speed, V_c, is equal to 30 m/min and the depth of cut, h, is 0.28 mm.

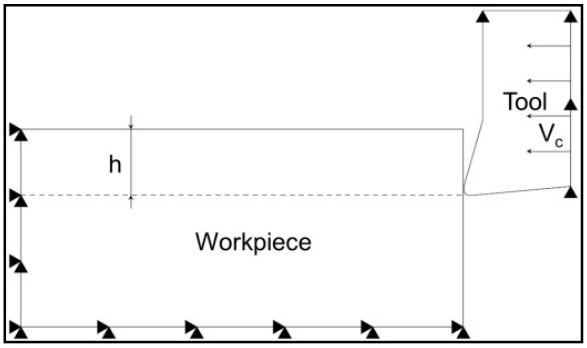

Fig. 1. Initial geometry and boundary conditions of the model

The tool material is tungsten carbide and its behavior is described by a linear elastic law. The workpiece material is Ti6Al4V. Taking strain softening into account is necessary to produce saw-toothed Ti6Al4V. The Hyperbolic TANgent (TANH) model introduced by Calamaz et al. [2] is used to describe the workpiece material behavior. The TANH law is a Johnson-Cook law modified in order to model the strain softening effect. The Ti6Al4V metallurgical state for which Calamaz et al. identified the TANH law is not known. This is a source of difference with our experiments.

An explicit Lagrangian formulation is adopted as the model must be able to deal with the absence of chip generation and the transient phase of the chip formation, as highlighted in [1].

Due to the Lagrangian formulation, a damage criterion based on an 'eroding element' method is introduced in the model to make chip formation possible. This separation criterion is based on the temperature dependent tensile failure of Ti6Al4V. As soon as the tensile failure value is reached in a finite element, it is deleted from the visualisation and all of its stress components are put to zero. The suppression of a finite element introduces a crack in the workpiece, making it possible for the chip to come off.

Coulomb's friction is used to model friction at the tool – chip interface and all the friction energy is converted into heat, which is usually assumed [3]. The workpiece and tool initial temperature is set to 25°C. Only conduction is considered and all the parts faces are adiabatic.

3. Experiments presentation

Experiments were performed on a lathe with the same cutting parameters as the numerical model in orthogonal cutting conditions. The Ti6Al4V machined was annealed according to AMS 4928 [4].

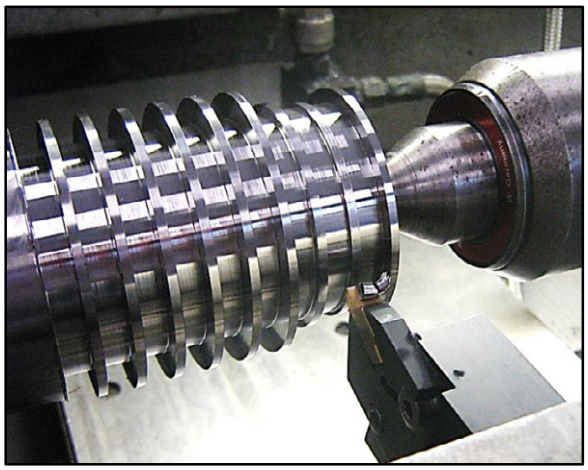

Fig. 2. Experimental setup

As shown on Fig. 2, the workpiece specimen is a shaft comporting flanges in the form of successive slices (diameter 60 mm) of equal thickness (2 mm). The tool and tool holder were custom made by SECO in order to provide the same characteristics as the numerical model. The tool width (6 mm) is larger than that of the disks to satisfy plain strain conditions. The cutting process is performed in a plunge cutting mode on each slice in dry cutting conditions. The tool was fixed on the lathe in a way to provide a high rigidity, particularly in the cutting direction and forces were measured with the 9257B Kistler dynamometer. The chips were collected to be observed later on an optical microscope. In order to avoid workpiece displacements and vibrations a tailstock was used.

4. Comparison with experimental results

Experimental chips were etched and polished before observation with an optical microscope. For the cutting conditions considered the chip is saw-toothed. A typical chip is presented on Fig. 3 (a). In order to characterize it three lengths are measured: the undeformed chip length L, the height of the teeth H and the valley C, highlighted on Fig. 4.

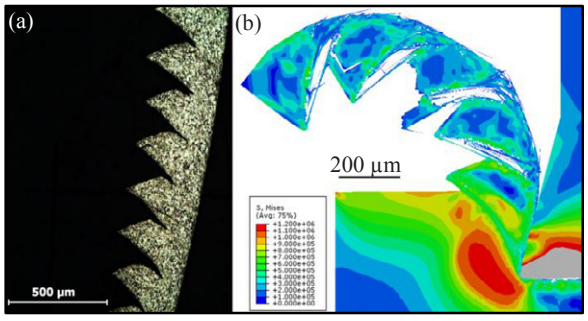

Fig. 3. Chip morphologies (a) experimental; (b) numerical

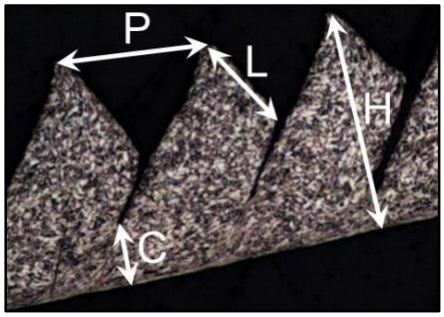

Fig. 4. Characteristics of a saw-toothed chip

The pitch P is also usually measured [5] but as the chip was unrolled for observation, this P value changes (more than H and C) and it will not be considered.

The numerical chip obtained is shown on Fig. 3 (b). Like the experimental one it is saw-toothed and its shape is qualitatively close to it. Two differences can be highlighted: numerical teeth are deeper and the second and third teeth contain a crack. The one of the third teeth is so long that it is broken. For the comparison it does not seem wise to take the first into account as the cutting regime is not yet established.

The three lengths are larger for the experimental chip. The valleys are very different (round 41%) and confirm the observations carried out on Fig. 3: numerical teeth are deeper than these of the experiments. The low tooth length (about 10% lower) coupled to the underestimated valley would mean that the teeth deformation is not sufficient and that the crack importance is too high in the chip formation mechanism.

Concerning the numerical chip formation mechanism, a strong deformation is observed in the primary shear zone and a crack propagates into it from its free surface to the tool. When analyzing the microstructure of the experimental chip, these features are also present. The chip formation mechanisms are therefore very close, meaning that the numerical model takes correctly into account the physical phenomena. It however seems that the crack propagates too easily in the model compared with the experiments.

Morphologies for other cutting conditions were also considered [6]. Saw-toothed (V_c = 75 m/min, h = 0.28 mm and V_c = 80 m/min, h = 0.163 mm) and nearly continuous (V_c = 6 m/min and V_c = 14 m/min, h = 0.19 mm) chips were obtained with numerical morphologies again qualitatively close to the experimental ones.

Experimental and numerical forces are presented on Fig. 5. The two cutting forces evolutions are cyclic, as expected for a saw-toothed chip. The five maxima identified for the numerical cutting force correspond to the five teeth of the chip. The magnitudes of the variation of the experimental forces are much more important than the numerical ones.

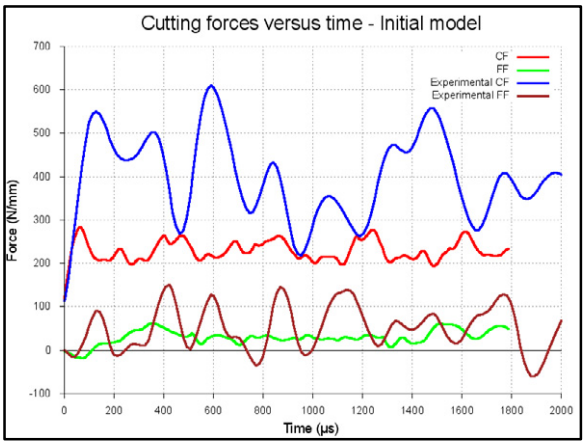

Fig. 5. Cutting forces with the initial model, low-pass filter cutoff frequency at 10 kHz

The RMS values of the forces are compared in Table 1. As it could be assumed from Fig. 5 the model largely underestimates the cutting force. The feed force is on the contrary very close to the experimental reference.

Table 1. RMS forces comparison

	Experiments	Initial	Modified	Final
CF (N/mm)	387	231	361	378
Difference (%)	–	40	7	2
FF (N/mm)	77	72	86	106
Difference (%)	–	7	-12	-38

As mentioned in the model presentation we have no precision on the Ti6Al4V metallurgical state used for the identification of the TANH law. Moreover depending on the law adopted the stresses vary greatly, leading to differences in the forces. At this point it is very likely that the TANH parameters do not correspond to our annealed Ti6Al4V.

5. Improvement of the cutting force

During the comparison between the experimental and the numerical chips, it has been shown that the mechanism of the chip formation is very close but the action of the crack seems to be too important (the teeth are deeper) and although having a cyclic evolution the numerical cutting force is too low. The main cause for this difference in the forces may be due to the different metallurgical state of the Ti6Al4V used to identify the TANH law.

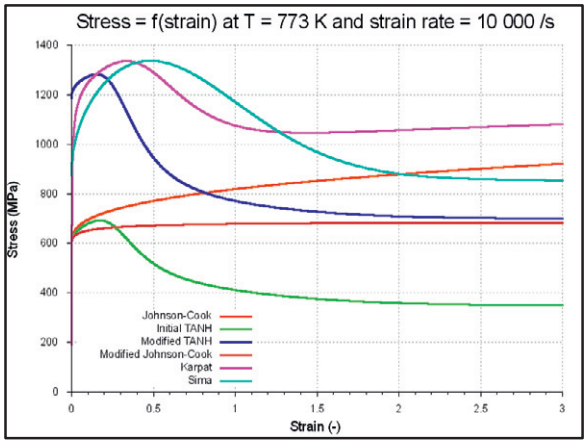

Fig. 6. Stresses evolutions

Therefore we propose to perform a first 'adaptation' of the model in order to bring the results closer to each others. The first step concerns the cutting force.

There exist many laws suitable to represent the behavior of a machined material. Fig. 6 shows four laws for Ti6Al4V taking the strain softening into account. When comparing the stresses at a fixed temperature and strain rate two groups of laws are identified: the first with the TANH [2] and modified Johnson-Cook [7] laws and the second with the Karpat [8] and Sima [9] law. At small strains, the stresses are nearly two times smaller for TANH law than for Karpat or Sima laws. The main reason for the difference between our experimental and numerical cutting forces could be there.

It is therefore proposed to pull the TANH curve up while maintaining its shape (the strain softening in particular). This 'level modification' is performed acting on the A parameter [2]:

$$\sigma = \left[A + B\,\varepsilon^{n}\left(\frac{1}{exp(\varepsilon^{a})}\right)\right]\left[1 + C\,ln\frac{\dot{\varepsilon}}{\dot{\varepsilon}_0}\right]$$

$$\left[1 - \left(\frac{T - T_{room}}{T_{melt} - T_{room}}\right)^{m}\right]\left[D + (1 - D)tanh\left(\frac{1}{(\varepsilon + S)^{c}}\right)\right]$$

with

$$D = 1 - \left(\frac{T}{T_{melt}}\right)^{d} \text{ and } S = \left(\frac{T}{T_{melt}}\right)^{b}$$

where σ is the flow stress, ε the plastic strain, $\dot{\varepsilon}$ the plastic strain rate, $\dot{\varepsilon}_0$ the reference plastic strain rate, T the workpiece temperature, T_{room} and T_{melt} are, respectively, the room and melting temperatures and a, b, c and d are material constants.

As the numerical cutting force is round 40% smaller than the experiments the value of A is doubled. The level difference between the original and the modified TANH laws is large and meets the expectations (Fig. 6). The curve is now closer to Karpat and Sima laws, the characteristics of each law still leading to distinct evolutions.

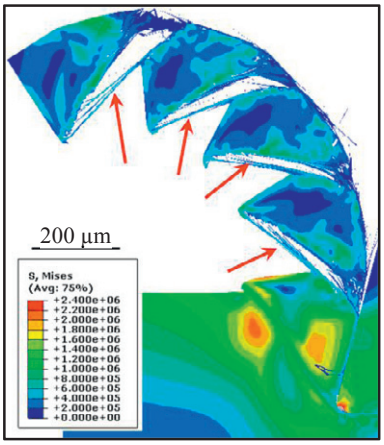

Fig. 7. Chip morphology of the modified model

Using the modified TANH law in the model should result in a higher cutting force thanks to larger stresses in the workpiece. It follows from this that the damage criterion must also be modified, the tensile failure value being reached faster. In consistency with the behavior law, the temperature dependent tensile failure values are also doubled.

The chip obtained with these modifications is presented on Fig. 7. It is still saw-toothed and composed of four fully formed teeth and a fifth one in formation. The morphology is close to the previous one (and therefore also to the experiments) and the teeth are well marked.

During the teeth formation some are detaching of the chip. It is caused by the conjunction of the crack progressing in the primary shear zone and a second one starting in the radius area of the tool. Some elements link two successive teeth (highlighted on Fig. 7) and it seems that the chip is still made of one piece. The drawback observed with the initial TANH law is therefore accentuated to the point of leading to a discontinuous chip (the valley can be considered equal to zero).

The main reason to modify the TANH law is that the cutting force is largely underestimated by the model. Fig. 8 shows that both forces are cyclic. As before feed forces are very close and the magnitude of the variations is smaller than experimentally. The repercussion of the TANH law modification on the cutting force is evident: its level is higher. It is now close to the experimental one. The magnitude of the variations is larger and gets closer to the experiments. The only notable difference between the two cutting forces is the width of the peaks, larger for the experimental case. It can be explained by

the removal of the teeth: it leads to a quick drop in the force and the tool has to move more to be again in contact with the workpiece and the force rises again.

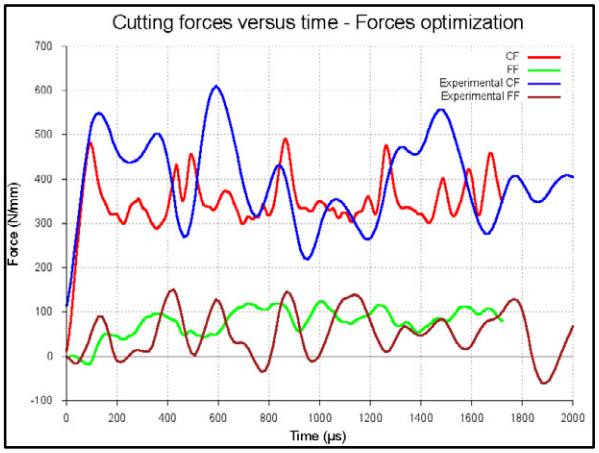

Fig. 8. Cutting forces with the modified model, low-pass filter cutoff frequency at 10 kHz

RMS values are compared in Table 1. The rise of the cutting force level is well translated in a higher RMS value. The difference between the experimental and numerical cutting and feed forces is very small. It is similar, even smaller, than the best results in literature for Ti6Al4V for other cutting conditions: 5%-10% for cutting force and 10%-15% for feed force [9-11].

As a conclusion of these modifications, the results are mixed. On one hand it is noted that the morphology of the chip is deteriorated: the problem identified in the initial model is amplified. The teeth are deeper again and a second crack appears, resulting in a chip formation mechanism moving away from the experimental one. On the other hand the level of the cutting force is now close to the experimental one. This increase was the main objective of the TANH law modification. The model fulfills therefore its role on this point. Lastly it is observed that when modifying the behavior and damage laws in the same proportions it is mainly the cutting force that is affected. The morphology is as well but in a less extent. The behavior law would therefore mainly acts on the level of the forces without affecting the morphology.

6. Improvement of the morphology

Following the conclusions of the first model modifications, only the morphology now needs to be improved to get closer to the experimental one.

For this second phase of the optimization the damage value is the parameter to look at. As the two previous models have shown that the crack propagates too quickly and easily, its value will be increased. Two modifications are considered: the first is tensile failure values 10% higher than in the previous model and the second is values 20% higher.

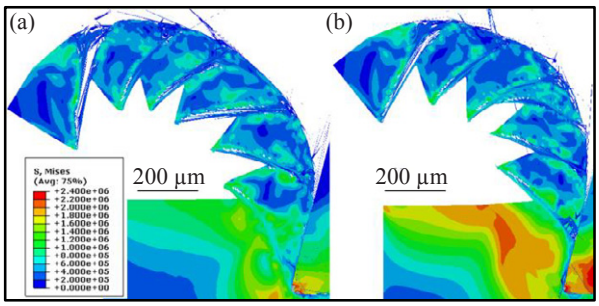

Fig. 9. Chip morphology (a) 10%; (b) 20% model

The two resulting chips are shown on Fig. 9. They are saw-toothed and quite similar. The first tooth is well marked, the others less. For the chip with the highest damage values, except for the first tooth, there is no crack in the primary shear zone, contrary to the other chip. The damage level might therefore be too high and the 10% higher case will be kept.

The three lengths measured on the previous chips were also on this one. Measuring the valley is not easy: micro-cracks are present in the primary shear zone of the third, fourth and fifth teeth without coming out of the free surface. The choice is to not take them into account, certainly resulting in an overestimation of this value (no micro-cracks were experimentally observed). The length and the height of the numerical teeth are still lower than experimental values (about 27% and 25%). The valley is now larger by round 30%, which is a maximum (and an overestimation).

As for the experiments the numerical chip formation results of deformation and crack propagation. It is noted that for some teeth (mainly the second and the fifth) a second crack also appears in the cutting edge radius area. It is similar to the one observed for the first model with the modified TANH law. This drawback is therefore not completely eliminated. The rise of the damage value does not solve the problem (or at least in the proportions used here): the fifth tooth of the 20% higher model has also a crack like this. There is however no cracks in the teeth as in the first model, which is an improvement.

Table 1 compares the RMS values. For the cutting force they can be considered as identical. Such results are not found in literature. The feed force is higher than for the previous model, increasing its difference with the experimental value.

7. Conclusions

The main outline of this paper is the partial decoupling between the morphology and the forces at least within the limits of the variations selected. Indeed, their level is mainly influenced by the behavior law while damage acts mostly on the chip morphology. Therefore it turns out that it is possible to modify one without greatly impacting the other.

Modifications of the TANH law can be justified by the initial difference between it and other laws found in literature as Kartpat's or Sima's. Concerning damage, physical meaning must be used as no data are available to compare to the modified criterion.

The final results are very satisfying. The cutting force is close to the measured one, the morphology is similar to these of the experimental chip and the formation mechanism implies deformation and crack propagation in both cases. The feed force is on the contrary overestimated. The parasitical cracks observed in some teeth are not present anymore but others smaller appear in the primary shear zone near the cutting edge radius area. Micro-cracks are also observed in the primary shear zone for the numerical chip, none were identified during the experiments. The teeth are not too deep anymore and the valley value is closer to the experimental one.

Acknowledgements

The authors gratefully acknowledge the FEDER financial support (SINUS project) allowing to carry out the experimental tests.

References

[1] Ducobu, F., Rivière-Lorphèvre, E., Filippi, E., 2011. A Lagrangian FEM Model to Produce Saw-toothed Macro-chip and to Study the Depth of Cut Influence on its Formation in Orthogonal Cutting of Ti6Al4V, Advanced Materials Research 223, p. 3.

[2] Calamaz, M., Coupard, D., Girot, F., 2008. A new material model for 2D numerical simulation of serrated chip formation when machining titanium alloy Ti-6Al-4V, International Journal of Machine Tools and Manufacture 48, p. 275.

[3] Nasr, M., Ng, E.G., Elbestawi, M., 2007. Effects of workpiece thermal properties on machining-induced residual stresses – thermal softening and conductivity, Proceedings of the IMechE, Part B: Journal of Engineering Manufacture 221, p. 1387.

[4] ASM Handbook Committee, 1990. Metals Handbook – Properties and Selection: Nonferrous Alloys and Special-Purpose Materials, volume 2, ASM International, 10th edition.

[5] Umbrello, D., 2008. Finite element simulation of conventional and high speed machining of Ti6Al4V alloy, Journal of Materials Processing Technology 196, p. 79.

[6] Ducobu, F., 2013. Contribution to the study of Ti6Al4V chip formation in orthogonal cutting. Numerical and experimental approaches for the comprehension of macroscopic and microscopic cutting mechanisms, Ph.D. Thesis, UMONS.

[7] Calamaz, M., Coupard, D., Nouari, M., Girot, F., 2011. Numerical analysis of chip formation and shear localisation processes in machining the Ti-6Al-4V titanium alloy, International Journal of Advanced Manufacturing Technology 52, p. 887.

[8] Karpat, Y., 2009. "Finite element modeling of machining titanium alloy Ti-6Al-4V using a modified material model", 12th CIRP Conference on Modeling of Machining Operations. San Sebastian, Spain, p. 107.

[9] Sima, M., Özel, T., 2010. Modified material constitutive models for serrated chip formation simulations and experimental validation in machining of titanium alloy Ti-6Al-4V, International Journal of Machine Tools and Manufacture 50, p. 943.

[10] Karpat, Y, 2011. Temperature dependent flow softening of titanium alloy Ti6Al4V: An investigation using finite element simulation of machining, Journal of Materials Processing Technology 211, p. 737.

[11] Zhang, Y.C., Mabrouki, T., Nelias, D., Gong, Y.D., 2011. Chip formation in orthogonal cutting considering interface limiting shear stress and damage evolution based on fracture energy approach, Finite Elements in Analysis and Design 47, p. 850.